

## Influence of Cavity Flow Regimes on Turbulence Diffusion Coefficient

Khan, M. I.\*<sup>1</sup>, Simons, R. R.\*<sup>2</sup> and Grass, A. J.\*<sup>2</sup>

\*1 Department of Chemical Engineering, The University of Birmingham, Edgbaston, Birmingham, B15 2TT, UK. E-mail: m.i.khan@bham.ac.uk

\*2 Civil and Environmental Engineering Department, University College London, Gower Street, London, WC1E 6BT, UK.

Received 25 December 2004  
Revised 20 July 2005

**Abstract**: Skimming, wake interference and isolated roughness flow regimes were investigated in the cavity formed between 2-d roughness elements in a laboratory water flume. The flow direction was aligned perpendicular to the roughness elements. Flow visualization and laser Doppler velocimetry were used to confirm the flow pattern and corresponding turbulence characteristics of the flow. Influence of the flow regimes on Reynolds stresses and turbulent diffusion coefficient was investigated at roof level of the cavity. Sweep events towards the wall were significantly affected by the rough bed. A relatively wider cavity demonstrated significant influence on ejection and sweep stresses because of vortex activity at upstream and downstream positions within the cavity. The turbulent diffusion coefficient increased for isolated roughness flow in comparison to skimming flow regime.

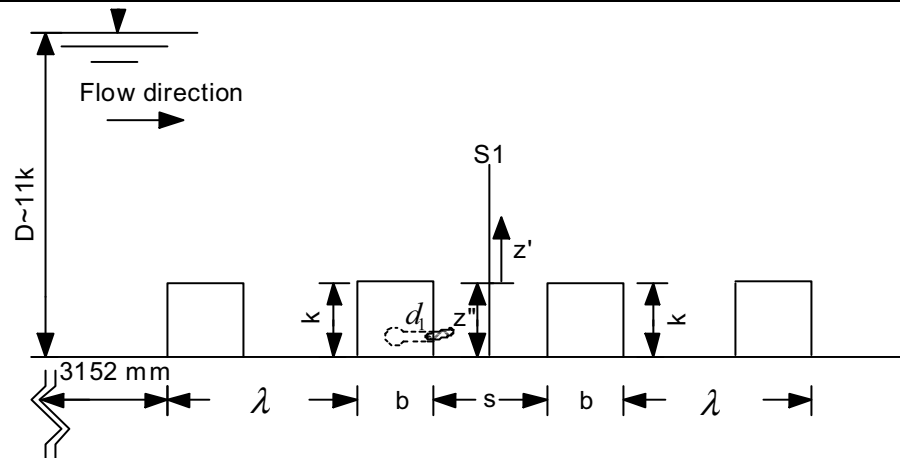
**Keywords**: Turbulence diffusion, Mixing length scale, Bed roughness, Flow pattern.

### 1. Introduction

For flow over 2-d roughness elements, the importance of gap ( $s$ ) to height ( $k$ ) ratio of the roughness array for the separation and reattachment of the stream lines in the canyon between the elements has been noted by many researchers. Surface roughness can be classified between ' $k$ ' type ( $s \geq 3k$ ) and ' $d$ ' type ( $s \leq k$ ) according to Perry et al. (1969), who made a comparison between the ' $k$ ' and ' $d$ ' type roughness by adjusting the spacing to produce the required roughness behaviour. In the case of ' $k$ ' type roughness,  $k$  is the controlling parameter. Eddies with a length scale proportional to  $k$  are shed into the flow above the crests of the elements. In the second, i.e., the ' $d$ ' type roughness, the flow within these cavities between the elements is largely self contained, being separated from the outer flow by a shear layer across the top of the cavity. Such a flow behaviour was termed "skimming flow". The variation in 2-d roughness geometry was found by Oke (1987) to generate three kinds of flow pattern. These were referred to as isolated roughness flow, wake interference flow and skimming flow. The roughness geometry was characterised by its aspect ratio, which is the height ' $k$ ' of the canyon divided by gap width between adjoining elements ' $s$ '. For wide canyons ( $s/k > 3.33$ ), the roughness elements are well spaced and act essentially as isolated roughness elements. As roughness become more closely spaced ( $3.33 > s/k > 1.53$ ), the disturbed flow has insufficient distance to readjust. In the case of skimming flow ( $s/k < 1.53$ ), the bulk of the flow skims over the canyon.

Table 1. Idealised 2-d bed roughness geometry in water flume tests (see Fig. 1).

Test	Gap distance (mm) $s$	$s/k$	Remarks Roughness Geometry:
1	7.5	1.5	$k = 5 \text{ mm}$ and $b = 5 \text{ mm}$ (Fig. 1)
2	20	4	
3	45	9	

Fig. 1. A schematic of the 2-d slat type roughness geometry showing the dye injection position  $d1$ .

Theodorsen (1952) was the first to postulate the turbulent boundary layer is made of coherent eddy structures or vortex loops also variously referred to as 'horseshoe' or 'hairpin' vortices. Kline et al. (1967) observed a gradual uprising of the low speed streaks towards the external region of the boundary layer. During an ejection, jets of low streamwise momentum are observed to be ejected away from the wall region into the outer flow. On the other hand, jets of high streamwise momentum directed towards the wall and are generally described as an "inrush" or "sweep" event. Grass (1971) from his experiments in a water flume found that ejection and inrush events form part of a randomly occurring yet linked cyclical process of turbulence generation in the boundary layer which has been shown to be responsible for most of the turbulence energy production and major contribution to the Reynolds stress momentum transport in the wall layers. Schoppa and Hussain (2000) suggested a cycle was controlling the wall turbulence in which low speed streaks are considered responsible for the initial generation of vortices, which in turn generate the ejection and sweep events. Eames and Gilbertson (2004) reported that these coherent vortical structures generate regions of significant strain and are the primary agents for dispersing and mixing particles.

In this paper the influence of cavity flow regimes was investigated on the ejection and sweep events and the turbulence diffusion coefficient using laser Doppler velocimetry and flow visualization techniques.

## 2. Experimental Setup

### 2.1 Open Channel Flume

A re-circulating water flume with overall physical dimensions 6.2 m long, 0.5 m wide and 0.3 m high glass side walls was used for experimental work. A glass bed, 0.495 m wide and 4m long was laid in the flume over levelled sleepers on the marine plywood channel base to obtain a closely horizontal bed. At the inlet of the channel, a specially designed brass leading edge was followed by a fairing which led to a short length (75 mm) of smooth bed. In order to avoid the formation of a local separation bubble, the surface of this smooth bed section was laid flush with the crest height of the roughness elements. A schematic of the 2-d slat type roughness geometry is shown in Fig. 1. For flow visualization tests, injector  $d1$  was used to allow dye to be introduced into the flow 1.5 mm above the glass bed to facilitate the study of dispersion. The roughness elements were formed from

lengths of 5 mm (nominal) square brass bar, spanning the width of the flume and extending over the 4m length of the levelled glass bed. The cavity aspect ratio was investigated for the  $s/k$  ratios shown in Table 1. Attachment of the roughness elements to the glass plate was by means of double sided adhesive tape, and particular attention was paid to the cleanliness of the mating surfaces in order to ensure firm adhesion. The actual dimensions of the elements therefore showed a mean variation of  $\pm 1.25\%$  over the nominal 5mm dimensions. The flow depth was kept constant by altering the bed slope in order to maintain a uniform flow.

## 2.2 Measurement Technique

Behaviour of the flow inside the cavity formed between the roughness elements was visualized with Rhodamine-6G solution. This dye when illuminated with the output of an argon ion laser gave dark red and yellow colours which helped in visualizing the flow pattern inside the cavity.

A two-component laser Doppler velocimeter (LDV) was employed for quantitative measurements of instantaneous velocities around the test cavity at section marked S1 in Fig. 1. The measurement volume diameter of the LDV in streamwise direction was 90.5 micron and length across the flume was 1.31 mm. The signals were processed using TSI IFA655 signal processors with FIND software. The processors were operated in coincident mode to ensure that measurements of both horizontal and vertical velocity components were made for the passage of each seeding particle detected.

## 3. Results

### 3.1 Flow Pattern Observation

The flow pattern in the cavity between the roughness elements can be classified as skimming, wake interference and isolated roughness flow.

#### 3.1.1 Skimming Flow

In skimming flow the roughness elements are relatively closely spaced, the bulk of the mean flow does not enter the cavity (or canyon) and a stable vortex is established in the cavity, as shown in Fig. 2a and 3a. The skimming flow regime has been identified with the help of flow visualization. The flow visualization results (Fig. 2a) using a laser light sheet showed an organised single vortex flow in the cavity. The formation of the vortex inside the cavity between the roughness elements was also confirmed by the LDV measurements shown in Fig. 3a. On the basis of flow visualization, it was found that an organised 2-d vortex flow is present for a gap to height ratio ( $s/k$ ) of 1.5.

#### 3.1.2 Wake Interference Flow

Wake interference flow is one in which the two vortices formed inside the cavity, one at the upstream and the other at the downstream corners, interact strongly with each other as shown in Fig. 2b and 3b. The LDV measurements provided evidence for the increase in local mean streamwise velocity inside the cavity with the increase in gap distance between the roughness slats as conditions changed from skimming to wake interference flow (see Fig. 4). The change in cavity flow pattern has a significant influence on the increase in streamwise and vertical turbulence fluctuations shown in Fig. 5 and 6 respectively.

#### 3.1.3 Isolated Roughness Flow

Isolated roughness flow occurs when the roughness elements are well apart. The flow is classified as isolated roughness flow when the upstream vortex acts independently of the downstream vortex inside the cavity. Multiple horizontal vortices form between the roughness elements. The reverse flow at the centre of the cavity becomes negligible and turbulence fluctuations stay high. As the vortices change their position inside the cavity (Fig. 2c and 3c) they become more able to interact with the outer boundary layer. This interaction has a direct effect on the gradual increase in Reynolds stresses shown in Fig. 7 for  $s/k = 1.5$  to  $s/k = 9$ . As a consequence there is an increase in boundary layer turbulence production, which facilitates the dispersion of the pollution from the street canyon.

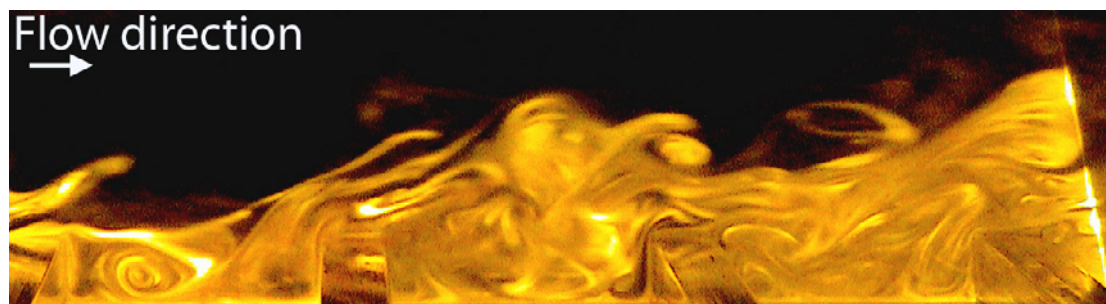
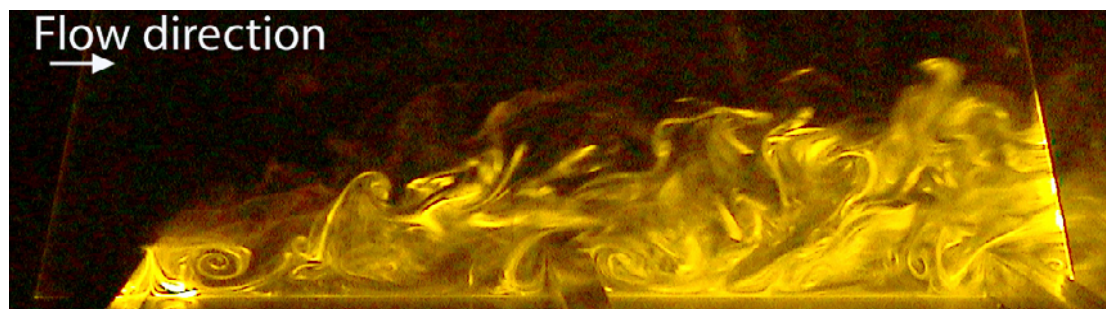
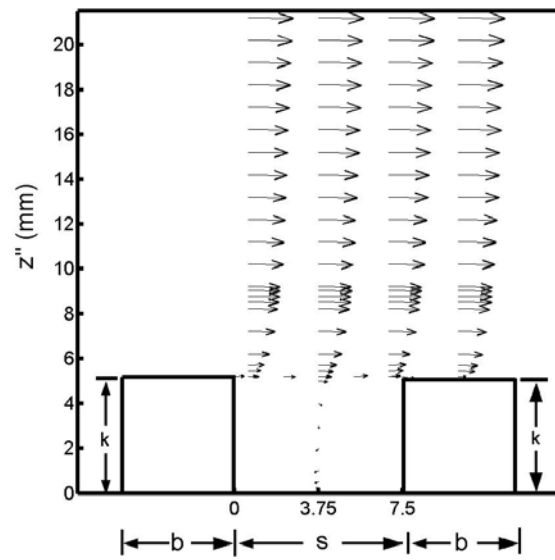
a) Skimming flow visualization for gap distance  $s/k = 1.5$  between slatsb) Wake interference flow visualization for gap distance  $s/k = 4$  between slatsc) Isolated roughness flow visualization for gap distance  $s/k = 9$  between slats

Fig. 2. Flow visualization with laser light sheet a) skimming, b) wake interference, c) isolated roughness flow.

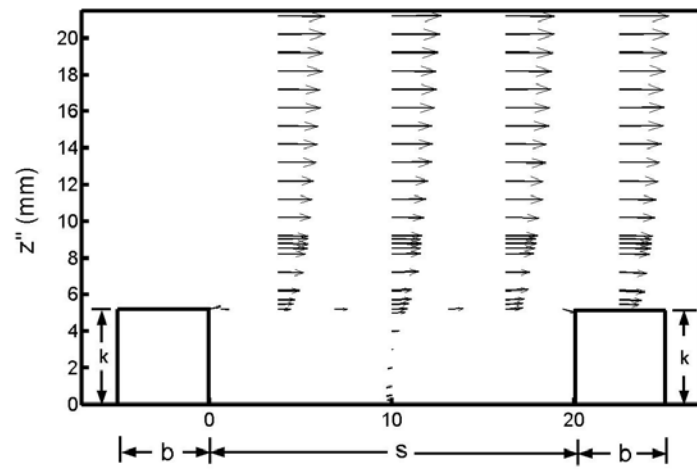
### 3.2 Quadrant Decomposition Technique

The interaction of the turbulent boundary layer with a rough surface has significant influence on the near wall coherent structures. These coherent structures are responsible for the production of the turbulent shear stresses, which contributed to the Reynolds stresses in the four quadrants of the  $(u, w)$  plane.

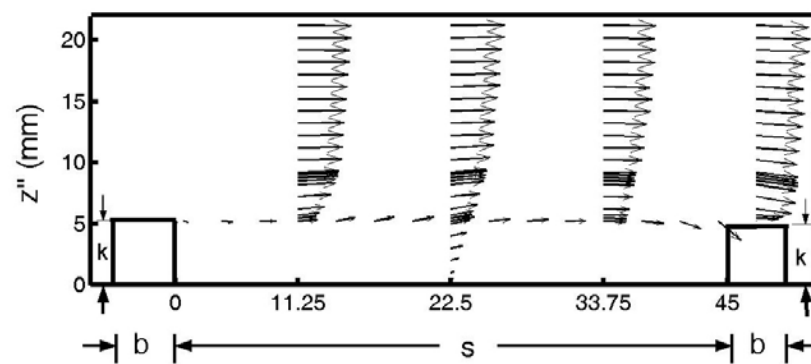
Analysis has been carried out similar to that performed by Lu and Willmarth (1973) in which the Reynolds stress at a point of the  $(u, w)$  plane is presented as a sum of the contributions measured in four quadrants of the  $(u, w)$  plane. During an ejection, the  $u' < 0$  and  $w' > 0$ , the corresponding point is located in the second quadrant ( $Q_2$ ). An ejection is detected when the point is located outside a hyperbolic hole of size  $H$ . The size of the hyperbolic hole determines the strength of the ejections and sweeps. Sweeps, with  $u' > 0$  and  $w' < 0$  can be detected in a similar way in the fourth quadrant ( $Q_4$ ). The contribution to the Reynolds stress determined in the  $Q_i$  quadrant outside the central region limited by four hyperbola is as follows:



a) Flow pattern for skimming flow over gap distance  $s/k = 1.5$  between slats



b) Flow pattern for wake interference flow over gap distance  $s/k = 4$  between slats



c) Flow pattern for isolated roughness flow over gap distance  $s/k = 9$  between slats

Fig. 3. Flow pattern from local mean flow velocities measured with LDV a) skimming, b) wake interference, c) isolated roughness flow.

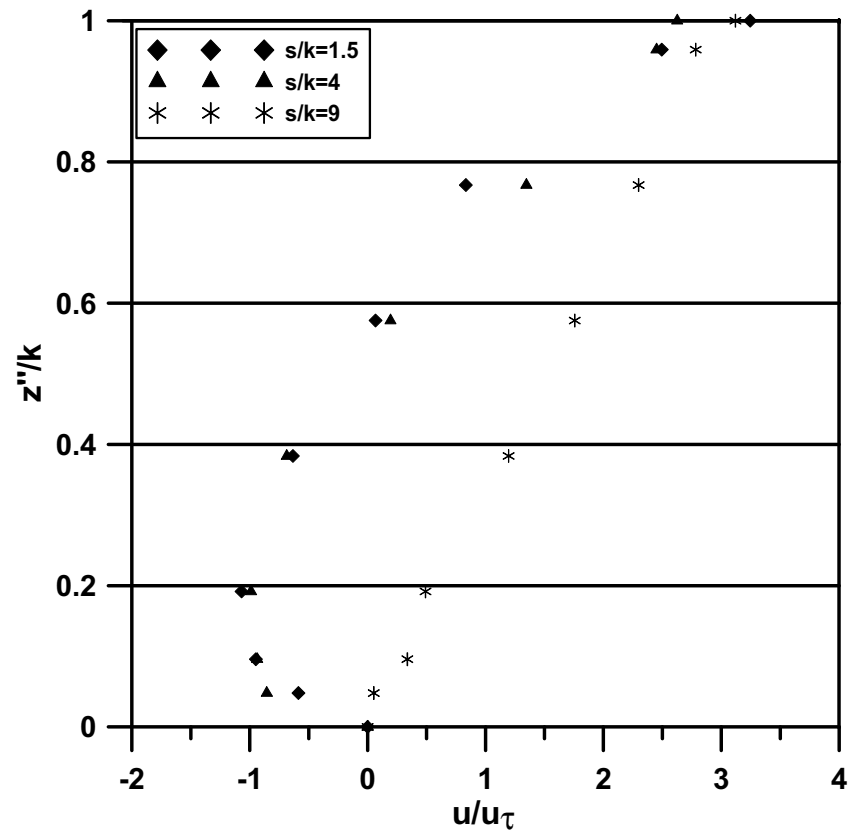


Fig. 4. Reverse mean flow velocity midway between roughness elements.

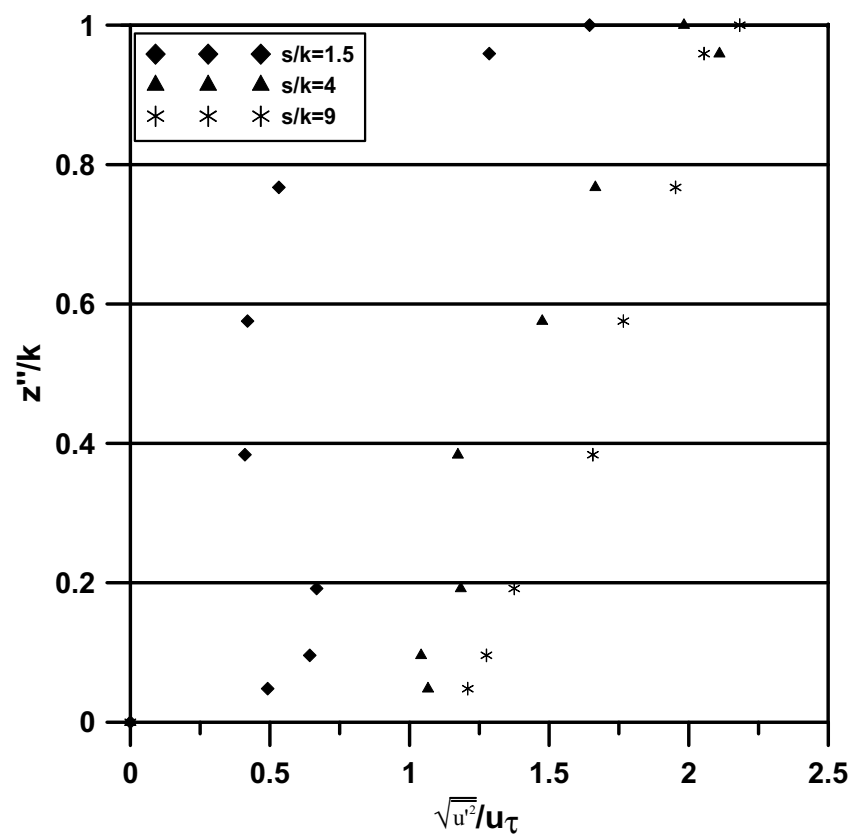


Fig. 5. Streamwise turbulence fluctuations midway between roughness elements.

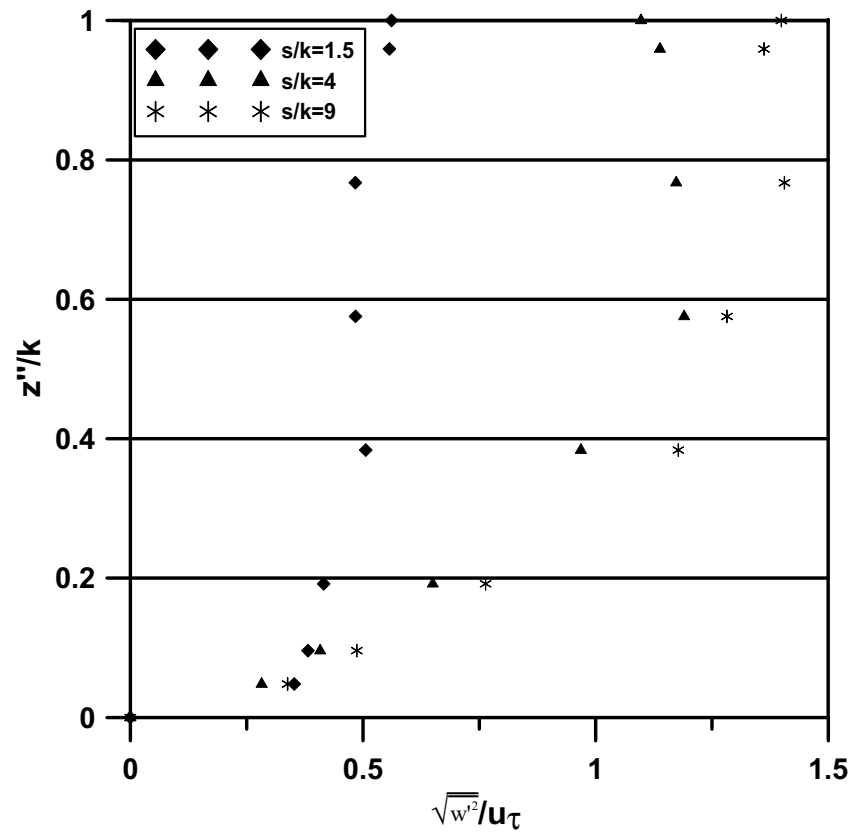


Fig. 6. Vertical turbulence fluctuations midway between roughness elements.

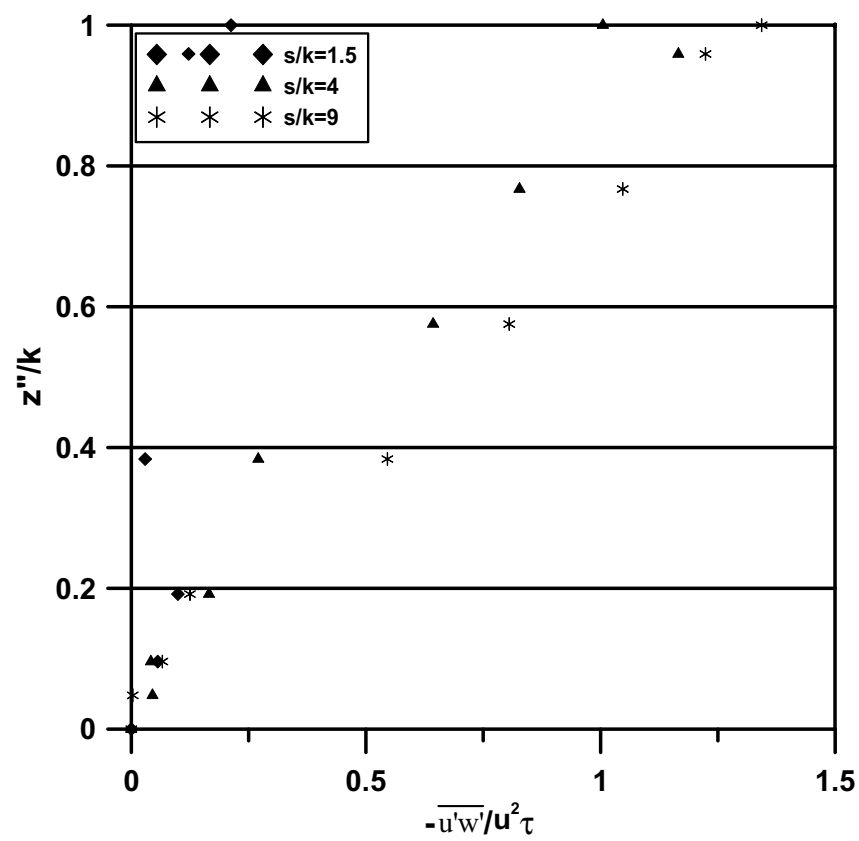


Fig. 7. Reynolds stresses midway between roughness elements.

$$\overline{(u'w')}_{\varrho_i} = \lim_{T \rightarrow \infty} \frac{1}{T} \int_0^T (u'w')_{\varrho_i} I dt$$

where  $I$  is the detection indicator function related to the occurrence of ejection and sweep events.

For an ejection event,  $I$  was defined so that  $\sqrt{u'^2}$

$$I = 1, \text{ If } u'w' < -H\sqrt{u'^2}\sqrt{w'^2} \text{ and } u' < 0$$

$$I = 0, \text{ Otherwise}$$

For a sweep, the detection indicator function  $I$  was defined so that

$$I = 1, \text{ If } u'w' < -H\sqrt{u'^2}\sqrt{w'^2} \text{ and } u' > 0$$

$$I = 0, \text{ Otherwise}$$

For the current paper, we have analyzed these phenomena for a value of  $H = 0$

The measurements of ejection to sweep ratio along the roof level at  $s/k = 1.5$  are shown in Fig. 8a. Slightly higher ejection to sweep ratio was found downstream in comparison to the upstream end of the cavity for skimming flow. Ejection to sweep ratios (Fig. 8b) for gap to height ratio ( $s/k$ ) of 4 show that the greater effective roughness enhanced the proportion of sweeps in comparison to the case with gap to height ratio ( $s/k$ ) of 1.5 (skimming flow) at the centre position of the cavity. For a wider cavity with  $s/k = 9$ , ejection to sweep ratio illustrated the presence of two active vortices, one upstream and the other at the downstream end of the cavity (Fig. 8c).

### 3.3 Mixing Length Scales and Turbulence Diffusion Coefficient

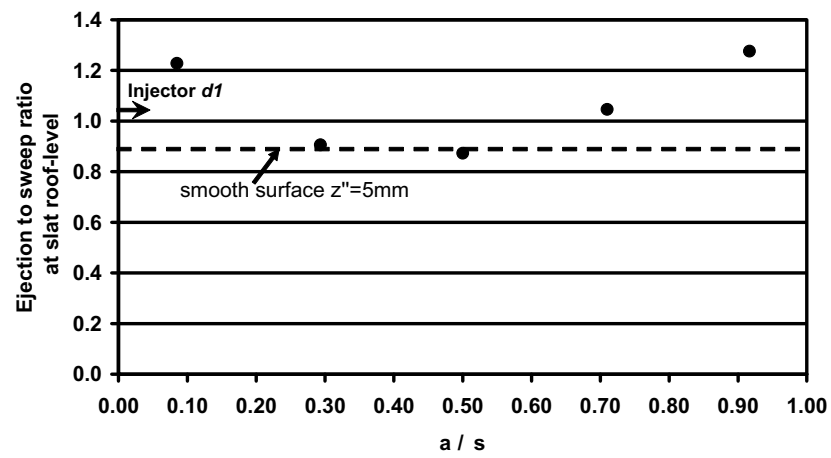
The results have been plotted in terms of Prandtl's (1925) mixing length theory (Fig. 9). The defining equation for mixing length  $l$  is obtained from,  $\frac{\tau_{wall}}{\rho} = l^2 \left(\frac{du}{dz}\right)^2$ . In Prandtl theory, expressions for  $u'$  and  $w'$  are obtained in terms of a mixing length distance  $l$  and the velocity gradient  $\frac{du}{dz}$ , where  $u$  is the temporal mean velocity at a point and  $z$  is the distance normal to the wall.

The mixing length scales in Fig. 9 were estimated using the distance above the top face of the roughness slats. They show the changes in  $l$  for a smooth surface through skimming flow and wake interaction to isolated roughness conditions for the 2-d slat roughness. In comparison to a smooth wall test, the mixing length scales were found to increase as the surface became rougher. The turbulent diffusion coefficient " $Cd$ " is not a material property of the fluid (unlike the coefficient of molecular diffusion) but depends upon the character of the turbulence. It can be expressed in the dimensional case as,  $Cd = \nu_w + V_T$ , where  $\nu_w$  is the kinematic viscosity of water and  $V_T$  is the turbulent viscosity. Sladek et al. (2004) reported the turbulence model which was employed for estimation of turbulent viscosity as,  $V_T = l^2 \sqrt{\left(\frac{du}{dz}\right)^2 + \left(\frac{dw}{dz}\right)^2}$ . Figure 10 illustrates that the turbulent diffusion,  $Cd$ , near the wall increases as the surface roughness increases. Taking kinematic viscosity of water to be  $1.004 \times 10^{-6} \text{ m}^2/\text{sec}$ , at roof level (position S1) the ratio of turbulent diffusion coefficient to molecular diffusion coefficient varied from 3 for skimming flow, to 9 for wake interference flow and 11 for isolated roughness flow regimes shown in Fig. 11.

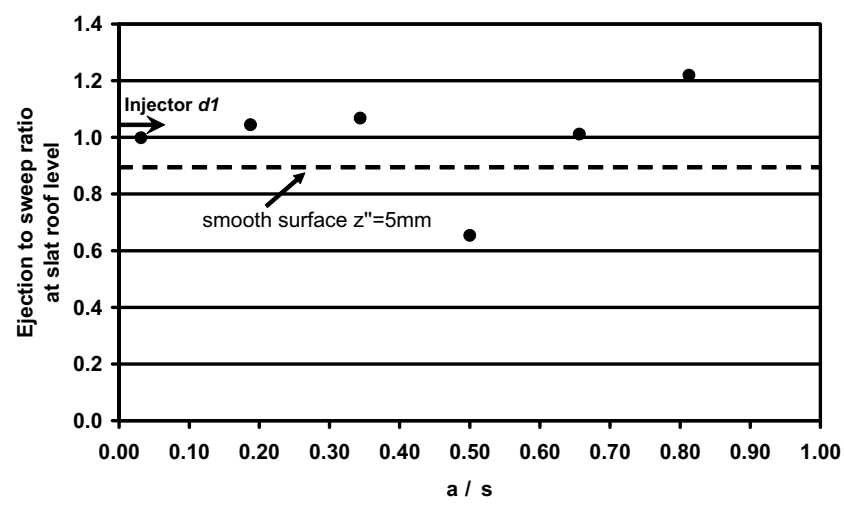
## 4. Conclusions

Flow in the cavity between the 2-d roughness elements is strongly affected by the aspect ratio ( $s/k$ ). From the hydraulic flume tests, it was possible to identify three flow regimes, namely, skimming, wake interference and isolated roughness flow. These results were in line with the reports of Oke

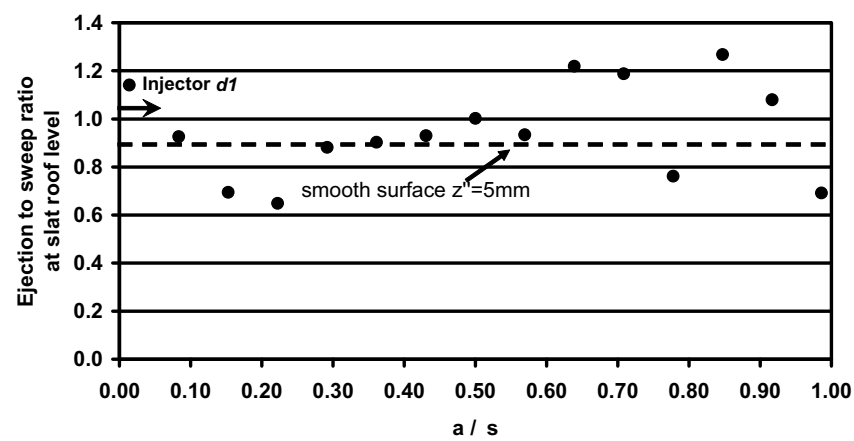




a) gap distance  $s/k = 1.5$



b) gap distance  $s/k = 4$



c) gap distance  $s/k = 9$

Fig. 8. Ejection to sweep ratios at  $z'' = 5\text{mm}$  along the gap between slats ( $H = 0$ ) a) skimming flow, b) wake interference flow, c) isolated roughness flow.

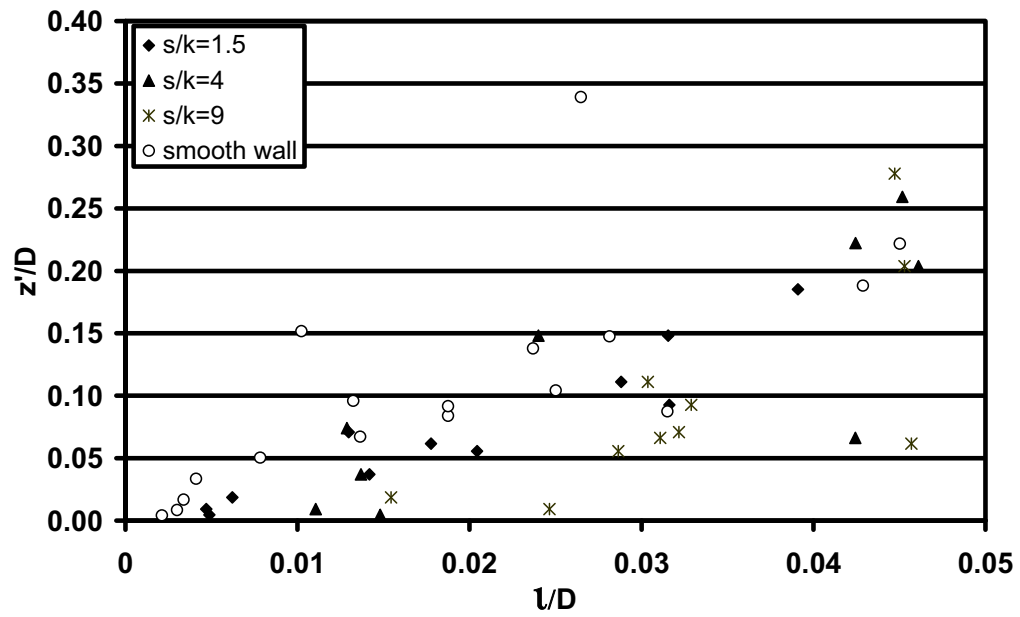


Fig. 9. Mixing length scale for flow regimes measured midway between roughness elements at S1.

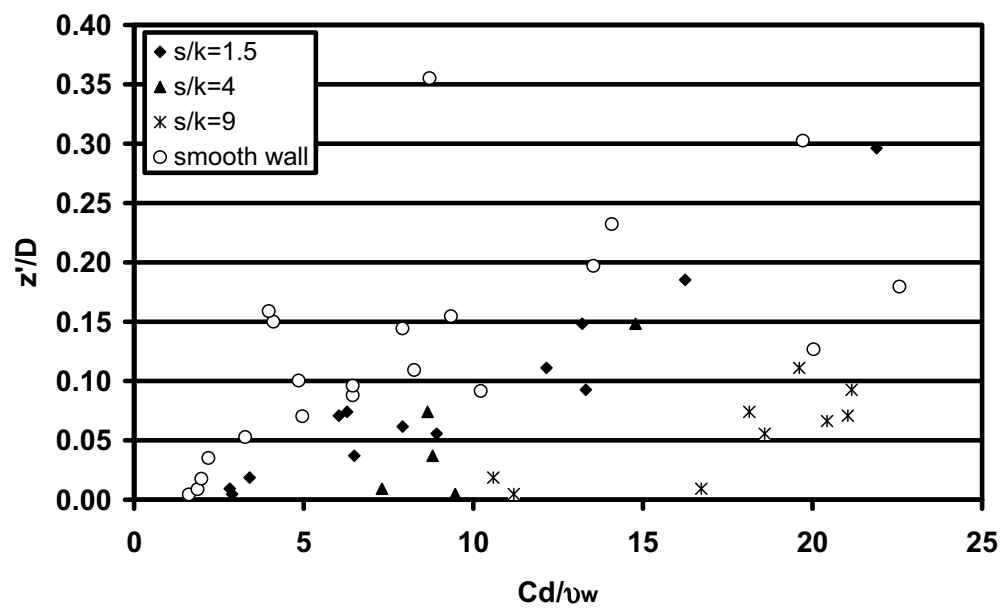


Fig. 10. Turbulent diffusion coefficient for flow regimes measured at position S1.

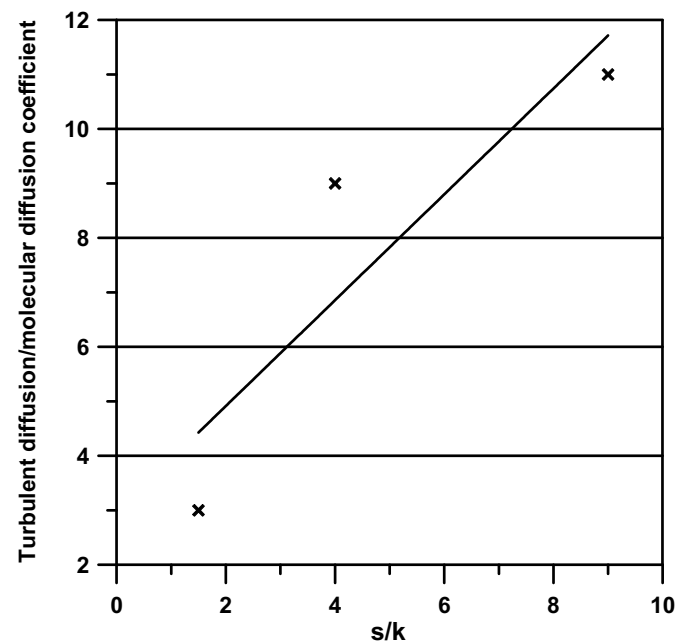


Fig. 11. Ratio of turbulent diffusion to molecular diffusion coefficient for flow regimes measured at roof level (position S1).

(1987), Sini et al. (1996), Huang et al. (2000) and Khan (2004). From the current tests it was found that the ejection and sweep events were common to skimming, wake interference and isolated roughness flow regimes. These random events are responsible for the transport of mass across the boundary layer. Dominant vortex activity was identified by significantly higher ejection and sweep events were observed in comparison to flow over a smooth wall. Sweeps associated with wake interference and isolated roughness flows were more significant in comparison to those in skimming flow. The increase in sweep events demonstrated the increase in turbulent behaviour of the flow. The turbulent diffusion characteristics for skimming, wake interference and isolated roughness flow regimes were governed by the turbulence generated because of variation in gap distance between the roughness elements.

### *Nomenclature*

$C_d$	Turbulent diffusion coefficient
$D$	Flow depth
$H$	Hyperbolic hole
$k$	Roughness element height
$\iota$	Mixing length scale
$s$	Gap distance between the roughness slats of model street canyon
$U(= u + u')$	Instantaneous stream wise velocity
$u'$	Fluctuating stream wise velocity component
$\sqrt{u'^2}$	Root mean square value for $U$
$u$	Local mean stream wise velocity
$\nu_w$	Kinematic viscosity of water
$W(= w + w')$	Instantaneous vertical velocity
$w'$	Fluctuating vertical velocity component

$\sqrt{w'^2}$	Root mean square value for W
w	Local mean vertical velocity
a	Streamwise position between the roughness elements
z'	Vertical distance from the roof level of roughness element
z''	Vertical distance from the wall to the roof level of the roughness element
$-\rho \overline{u'w'}$	Reynolds stress

### References

- Eames, I. and Gilbertson, M. A., The settling and dispersion of small dense particles by spherical vortices, *Journal of Fluid Mechanics*, 498 (2004), 183-203.
- Grass, A. J., Structural features of turbulent flow over smooth and rough boundaries, *Journal of Fluid Mechanics*, 50 (1971), 233-255.
- Huang, H., Akutsu, Y., Arai, M. and Tamura, M., A two dimensional air quality model in an urban street canyon: evaluation and sensitivity analysis, *Atmospheric Environment*, 36 (2000), Part 7, 1137-1145.
- Khan, M. I., The influence of two-dimensional bed roughness on the flow structure of a turbulent boundary layer, (2004), Ph.D. dissertation, University of London.
- Kline, S. J., Reynolds, W. C., Schraub, F. A. and Rundstadler, P. W., The structure of turbulent boundary layers, *Journal of Fluid Mechanics*, 30 (1967), Part 4, 741-773.
- Lu S. S. and Willmarth W. W., Measurements of the structure of the Reynolds stresses in a turbulent boundary, *Journal of Fluid Mechanics*, 60 (1973), 481-571.
- Oke, T. R., *Boundary layer Climates* (2<sup>nd</sup> Edition), (1987), 435, Rout ledge, London.
- Perry, A. E., Schofield, W. H. and Joubert, P. N., Rough-wall boundary layers in adverse pressure gradients, *Journal of Fluid Mechanics* 37 (1969), Part 2, 383-413.
- Schoppa, W. and Hussain, F., Coherent structure dynamics in near-wall turbulence, *Fluid Dynamics Research*, 26 (2000), 119-139.
- Sini, J. F., Anquetin, S. and Mestayer, P. G., Pollutant dispersion and thermal effects in urban street canyons, *Atmospheric Environment* 33 (1996), 4057-4066.
- Sladek, I., Kozel, K., Janour, Z. and Gulikova, E., In *Procs Int. Conf. On Urban Wind Engineering and Building Aerodynamics*, von Karman Institute, Belgium, von Karman Institute for Fluid Dynamics, (2004), C.9.1-C.9.10.
- Theodorsen, T., Mechanism of turbulence, 2<sup>nd</sup> Midwestern conference on Fluid Mechanics, Ohio State University, (1952), 1-18.

### Author Profile



Ijaz Khan: He received his Ph.D. degree in Fluid Mechanics at University of London in 2004. Later he joined the department of Chemical Engineering at University of Birmingham in 2005 as a research fellow. His current research interests are in computational fluid dynamics and laboratory scale model testing.



Richard Simons: After graduating from the University of Manchester in 1973 with a BSc (Hons) in Civil Engineering, he worked for Norwest Holst Ltd. In 1980 he was awarded a PhD in Fluid Mechanics at the University of London. He now works as a Senior Lecturer in the Department of Civil & Environmental Engineering at University College London. Current research interests are in coastal processes, wave-current interaction, turbulence, and boundary layer flows.



Anthony Grass: He is currently an honorary Emeritus Professor of Fluid Mechanics in the Department of Civil and Environmental Engineering at University College London, UK where he recently retired as the Head of the Fluid Mechanics Research Group. During a long academic career at UCL his research has focused on the dynamics and structure of turbulence in environmental boundary layer flows. Most recently in particular on the central role of coherent vortical structures and their influence on momentum and mass transport and mixing processes pertaining to sediment and pollutant transport in geophysical water and atmospheric air flows.